Magnetic Resonance Imaging 62 (2019) 121–128

Contents lists available at ScienceDirect

Magnetic Resonance Imaging

journal homepage: www.elsevier.com/locate/mri

Original contribution

A multivoxel pattern analysis framework with mutual connectivity analysis investigating changes in resting state connectivity in patients with HIV associated neurocognitve disorder

Adora M. DSouza[a,*], Anas Z. Abidin[b], Giovanni Schifitto[c,d], Axel Wismüller[a,b,d,e]

[a] Department of Electrical Engineering, University of Rochester, Rochester, NY, USA
[b] Department of Biomedical Engineering, University of Rochester, Rochester, NY, USA
[c] Department of Neurology, University of Rochester Medical Center, Rochester, NY, USA
[d] Department of Imaging Sciences, University of Rochester, NY, USA
[e] Faculty of Medicine and Institute of Clinical Radiology, Ludwig Maximilians University, Munich, Germany

ARTICLE INFO

Keywords:
Resting-state fMRI
Functional connectivity
Mutual connectivity analysis
BOLD fMRI
Machine learning
Feature selection

ABSTRACT

Functional MRI (fMRI) quantifies brain activity non-invasively by measuring the blood oxygen level dependent (BOLD) response to neuronal activity. It was recently demonstrated, on realistic fMRI simulations, that nonlinear connectivity approaches, such as Mutual Connectivity Analysis with Local Models (MCA-LM), are better suited for extracting connectivity measures than conventional techniques of cross-correlating time-series pairs. In this work, we investigate the application of MCA-LM in extracting meaningful connectivity measures aiding in distinguishing healthy controls from individuals presenting with symptoms of HIV Associated Neurocognitive Disorder (HAND), which occurs as a result of HIV infection of the central nervous system. The pairwise connectivity measures provide a high-dimensional representation of connectivity profiles for subjects and are used as features for classification. We adopt feature selection (FS) techniques reducing the number of redundant and noisy features, while also controlling the complexity of the classifiers. We investigate three FS techniques: 1) Kendall's τ, 2) Information Gain Attribute selection 3) ReliefF and two classifiers:1) AdaBoost and 2) Random Forests. Our results demonstrate that MCA-LM consistently outperforms correlation in terms of Area under the Receiver Operating Characteristic Curve and accuracy. Improved performance with MCA-LM suggests that such a nonlinear approach is better at capturing meaningful connectivity relationships between brain regions. This demonstrates potential for developing novel neuroimaging-derived biomarkers for HAND. Furthermore, FS helps identify connections between anatomical regions that are affected by HAND. In this work, we show that the regions of the basal ganglia and frontal cortex, which are known to be affected by HAND according to current literature, are identified as most discriminative.

1. Introduction

Signals measuring brain activity are obtained noninvasively using neuroimaging techniques like functional magnetic resonance imaging (fMRI). FMRI indirectly measures neural activity by quantifying the blood oxygen level dependent (BOLD) response to neuralactivity. Such a measure of brain activity is a complex function of cerebral blood volume, cerebral blood flow and the metabolic rate of oxygenation [1]. Connectivity analysis of fMRI data is carried out to uncover the underlying network structure of interactions between different regions in the brain. Recently, it was demonstrated that methods adopting state space reconstruction (SSR) from time-series data work well for estimating directed connectivity from realistic simulations of fMRI data [2]. This approach, originally formulated for estimating causal influences in complex ecological systems [3], uses delay-coordinate embedding to extract a measure of non-linear causation between time-series. Such an analysis called Mutual Connectivity Analysis with Local Models (MCA-LM) [4] profiles every individuals brain as a set of connections between individual voxels/regions, hence capturing the underlying dynamics of the resting brain. MCA [4] estimates a measure of nonlinear functional connectivity by estimating the mutual cross-prediction between pairs of neurophysiological time-series through SSR.

* Corresponding author at: Department of Electrical and Computer Engineering, University of Rochester, 500 Computer Studies Building, P.O. Box 270231, Rochester, NY 14627, USA.
E-mail address: adora.dsouza@rochester.edu (A.M. DSouza).

https://doi.org/10.1016/j.mri.2019.06.001
Received 5 December 2018; Received in revised form 9 May 2019; Accepted 2 June 2019

While fMRI sequences have been known to exhibit non-linear behavior in the presence of a stimulus [5,6] and at rest [7–9], majority of the literature on functional connectivity and multi-voxel pattern analysis (MVPA) [10] have focused on linear approaches, such as cross-correlation between time-series. In this work, we contrast the effectiveness of MCA-LM for representing the underlying dynamics in the brain with the more conventional approach of using functional connectivity analysis with correlation, in the MVPA framework.

MVPA was developed for predicting cognitive states of an individual recorded with fMRI when performing tasks in a scanner [10]. More recently, its applicability to resting-state fMRI has been demonstrated [11–14]. MVPA on resting-state data captures patterns of interaction between voxel time-series to predict disease state. Its framework consists of two steps: 1) To estimate measures of interactions between pairs of time-series as a connectivity matrix for every subject. 2) To quantify differences in connectivity between groups of subjects using machine learning techniques. Interest in MVPA methods to characterize and estimate discriminating features in brain connectivity of different subject groups has grown tremendously. It has been demonstrated to be effective in classifying patients with depression [12,15], and other psychiatric disorders [11,14,16–18]. The goal of our study is to investigate MCA-LM in the MVPA framework in quantifying differences in brain connectivity of subjects presenting with HIV Associated Neurocognitive Disorder (HAND) symptoms. Additionally, we compare performance with correlation, to estimate measures of connectivity from resting-state functional MRI (fMRI) sequences.

HAND is a co-morbidity associated with HIV infection due to the release of neurotoxic viral protein from infected microglia, non-productively infected glia cells and from perivascular infected/activated macrophages. This neurotoxic milieu is thought to lead to neuronal injury and dysfunction leading to clinically measurable cognitive impairment. However, these clinical diagnostic approaches do not reveal much about how neural connectivity within infected individuals is affected. Additionally, although neuropsychological tests aid in diagnosis of HAND once symptoms manifest, asymptomatic damage of the central nervous system go unnoticed at early stages of infection. Hence, there is a need for better diagnostic tools that are able to quantify changes in the brain function at early stages.

Recent work investigating neuroimaging derived bio-markers for detecting HAND with fMRI show promising results [19,20]. Furthermore, previous studies of subjects with HAND have demonstrated changes in connectivity of the default mode network, fronto-parietal network and basal ganglia [21–23]. In this work, in addition to learning a model that can distinguish between subjects with HAND and healthy controls, we investigate if MVPA with MCA-LM can potentially find neuroimaging-derived biomarkers and help identify underlying neural mechanisms for the symptoms of HAND. This is possible if predictions on out-of sample data are better than random implying that discriminative features are present in the neuroimaging data of the two subject groups.

In the following sections, we: 1) describe the patient population and the scanning parameters, 2) briefly discuss MCA-LM, feature selection techniques and classifiers adopted, 3) compare prediction quality upon using MCA-LM and correlation to generate connectivity matrices, and 4) investigate differences in connectivity measures between the two subject groups.

2. Materials

2.1. Participants

Subjects in this study were recruited as part of a NIH funded study (R01-DA-034977) at the University of Rochester Medical Center. Table 1 summarizes the demographic information of the subjects in this study. No significant differences in age between the two subject groups ($p > 0.05$) were observed. In total, 15 healthy controls and 14 HIV+ subjects with symptoms of HAND were recruited as part of this study. Of the subjects presenting with symptoms of HAND, 12 were diagnosed with Advanced Neurological Impairment (ANI) and 2 were diagnosed with Mild Neurological Deficit (MND). In HIV+ individuals, the absolute CD4 counts were 601 ± 395 cells/mm^3, whereas plasma viral load ranged from < 40/mL (undetectable) to 39,000 copies/mL. With the exception of one individual, all HIV+ subjects were on a stable cART regimen. Duration of HIV infection was calculated based on the time of initial HIV infection diagnosis. However, this may not reflect the true duration of the infection.

Table 1
Demographic characteristics for the population used in this study. The p-values indicate differences between control subjects and subjects presenting with HAND symptoms.

	Controls		Subjects with HAND symptoms		p-Value
	Mean	Std.	Mean	Std.	
Number	15		14		
Age	41.13	11.13	49.21	15.01	0.109
Gender (Male/Female)	8/7		10/4		
HIV duration (years)	N/A		10.98	9.28	
Viral load (log10)	N/A		1.85	1.77	
CD4 (cells/mm^3)	N/A		601.21	395.22	
Frame-wise displacement (FwD)	0.282	0.090	0.380	0.180	0.069

A standard battery of neuropsychological (NP) tests was used to assess cognitive abilities of subjects, covering six cognitive domains: executive function, speed of information processing, attention, memory, learning, and motor function. These scores were converted to age and education adjusted z-scores. An overall z-score combining the scores from individual domains was generated and used to assess HAND [24]. All participants provided written informed consent prior to participation as per protocol approved by the institutional IRB.

2.2. Resting-state fMRI data

Functional MRI scans were obtained from the subjects at the Rochester Center for Brain Imaging (Rochester, NY, USA) using a 3T, Siemens Magneton TrioTim scanner. The study protocol included: (i) High-resolution structural imaging using T1-weighted magnetization-prepared rapid gradient echo sequence (MPRAGE, TE = 3.44 ms, TR = 2530 ms, isotropic voxel size 1 mm, flip angle = 7°). (ii) Resting-state fMRI scans using a gradient spin echo sequence (TE = 23 milliseconds, TR = 1650 milliseconds, 96 *times* 96 acquisition matrix, flip angle of 84°). The acquisition lasted 6 min and 54 s, and 250 temporal scan volumes were obtained. A total of 25 slices, each 5 mm thick, were acquired for each volume. During acquisition, the subject was asked to lie down still with eyes closed. The data were acquired as part of a NIH sponsored study (R01-DA-034977).

Prior to computation of connectivity measures, the fMRI data used in this study was preprocessed using standard methodology. For each dataset, the first ten (of 250) volumes of functional magnetic resonance images were removed to analyze only those in which steady-state imaging had been reached. Next, motion correction, brain extraction and correction for slice timing acquisition were performed. Additional nuisance regression, was carried out to remove variations due to head motion and physiological processes. This model included linear and quadratic trends, signals from white matter and cerebrospinal fluid using and motion parameters. Studies have shown that functional connectivity measures may be affected by head motion [25,26] We compared head motion across the two groups using the average frame-wise displacement (FwD). No significant differences in FwD was observed between the two groups ($p > 0.05$, Table 1). Each dataset was finally registered to the 2 mm MNI standard space using a 12-parameter

affine transformation [27]. All preprocessing steps were carried out using the C-PAC software [28] and its corresponding dependencies in FMRIB Software Library (FSL) [29]. Finally, the time-series were normalized to zero mean and unit standard deviation to focus on signal dynamics rather than amplitude [30]. Based on the commonly used Automated Anatomic Labeling (AAL) template [31], the registered MRI volumes were divided into 90 regions (excluding the brain stem and cerebellar regions), 45 in each hemisphere. The cerebellar regions was not included in this study since it is generally spared from the effects of this disease [32,33] and it has been observed that HIV related impairment exists primarily in the Fronto-Striato-Thalamo-Cortical circuits and centers predominantly controlling executive functioning [34,35]. A representative time-series for each region was computed by averaging the time-series of all voxels within it.

3. Methods

3.1. Constructing connectivity profiles

3.1.1. Mutual connectivity analysis with local model

Nonlinear data-driven approaches applied on fMRI data do not assume prior knowledge about the model driving a system and capture the signal dynamics without explicitly modeling the hidden neuronal state. Mutual Connectivity Analysis (MCA) [4] with local models (MCA-LM) [2] establishes a measure of nonlinear association between every pair of time-series in a system. For every subject, these measures are represented as a connectivity matrix, quantifying the underlying dynamics of their resting brain. Here, we study the effectiveness of quantifying non-linear dynamics in extracting relevant information about connectivity in the resting human brain, thereby characterizing patterns in fMRI data useful to distinguish the two subject groups.

Consider a system with two time-series, **x** and **y**, sharing a manifold [36–38] which represents the system state space. If **y** influences **x**, estimates of the states of **y** can be obtained from that of **x**, but not vice versa, unless **x** influences **y** [3]. A measure of causation is established with local models, where the signature of the influencing time-series **y** is looked for in the influenced series **x**. This is done by quantifying the correspondence between the libraries of nearby points in the attractor manifold built from **x** to that built from **y**. To put this simply, the prediction quality of **x** cross-predicting **y** measures the influence **y** has on **x** [3].

This approach uses local models to detect influences derived from time delay-coordinate embedding methods. With delay-coordinate embedding, time-series **x** is represented as a manifold $\boldsymbol{M}_{\mathbf{x}}$ of dimension d. $\boldsymbol{M}_{\mathbf{x}}$ is constructed using vectors $\mathbf{x}_t = [x(t-(d-1)), \ldots, x(t-1), x(t)]$, and $t \in d, \ldots, T$. To obtain a cross-prediction of **y** using states of **x** denoted as $\hat{\mathbf{y}}|\boldsymbol{M}_{\mathbf{x}}$ at a point t, i.e. $\hat{y}(t)|\boldsymbol{M}_{\mathbf{x}}$, we obtain the $d+1$ nearest neighbors of $\boldsymbol{x}_t$, whose time-indices are used to identify nearest neighbors of $y(t)$ and obtain an estimate $\hat{y}(t)|\boldsymbol{M}_{\mathbf{x}}$ as follows:

$$\hat{y}(t)|\boldsymbol{M}_{\mathbf{x}} = \sum_{i=1}^{d+1} w_i y(t_i) \tag{1}$$

The cross-predicted estimate of $\hat{y}(t)|\boldsymbol{M}_{\mathbf{x}}$ is established with weighted average local models to detect non-linear dynamics derived from time delay-coordinate embedding. The weights w_i ($i \in \{1, \ldots, d+1\}$), are determined bya softmax function, such that the first nearest neighbor $\mathbf{x}_{t_i}$ of $\mathbf{x}_t$ has the highest weight,

$$w_i = \frac{e^{-\|\boldsymbol{x}_t - \boldsymbol{x}_{t_i}\|^2 / \|\boldsymbol{x}_t - \boldsymbol{x}_{t_1}\|^2}}{\sum_{j=1}^{d+1} e^{-\|\boldsymbol{x}_t - \boldsymbol{x}_{t_j}\|^2 / \|\boldsymbol{x}_t - \boldsymbol{x}_{t_1}\|^2}} \tag{2}$$

If **y** influences **x**, the nearest neighbors of $\boldsymbol{M}_{\mathbf{y}}$ correspond to those of $\boldsymbol{M}_{\mathbf{x}}$, and hence a good estimate of **y** is obtained. The similarity measure between the estimated $\hat{\mathbf{y}}|\boldsymbol{M}_{\mathbf{x}}$ and the original time-series **y** is estimated by correlating the two time-series. This quantifies the ability of **x** to cross-predict **y**. This measure quantifies a directed non-linear criterion of interaction, which is stored in a connectivity matrix **S** at matrix element $\mathbf{S}_{(\mathbf{x},\mathbf{y})}$. In a similar manner, a measure of cross-prediction between every time-series pair is obtained. Further details can be found in [3].

3.1.2. Functional connectivity using Pearson's correlation

Correlation measures the linear statistical association between two time-series. We compare patterns of connectivity obtained using MCA-LM with conventionally used correlation-derived measures. This is performed by correlating every low pass filtered time-series with each other. They time-series were filtered to the band 0.01–0.1 Hz to reduce physiological noise. However, with MCA-LM the step of filtering the data can be eliminated since MCA-LM can pick up higher order, non-linear interactions [3] that simpler methods such as cross-correlation cannot.

3.2. Multivoxel pattern analysis

MCA-LM and correlation produce connectivity profiles conveying different information about regional time-series interaction. The connectivity matrices are vectorized (after symmetrizing MCA-LM matrices) such that each subject is represented as an $N(N-1)/2$ feature vector where $N = 90$, where N is the number of regions defined by the AAL template.

3.2.1. Feature selection

Features correspond to measures of interaction between every pair of regions in the brain, obtained from connectivity analysis. Feature selection aims at extracting those interactions that best discriminates controls from subjects with HAND; hence identifying connections most relevant to the task of classifying the two populations. Additionally, feature selection eliminates noisy irrelevant features, and reduces the computational complexity of a classifier. Feature selection was performed independently for every set of training/test set split. In this study, we investigate three different feature selection approaches. Feature ranking estimated by the different feature selection approaches was used to select s features where $s \in \{2, 3, 5, 8, 10, 15, 20, 25, 50, 80\}$.

Kendall's τ coefficient:

Kendall's τ coefficient [39] ranks each feature by its relevance to the classification task by performing a test of independence between variables of different classes for every feature. The rank of each feature f is given by the magnitude of τ_f, where τ_f is given by:

$$\tau_f = \frac{n_c - n_d}{m_p \times m_h} \tag{3}$$

Here, m_p is the number of positive subjects (subjects with symptoms of HAND), m_h is the number of healthy controls, n_c is the number of concordant pairs and n_d is the number of discordant pairs. The total number of sample pairs is $m_p \times m_h$, since the relationship between instances belonging to the same group is not considered.

For attribute f and classes c_a and c_b for two instances, a_f and b_f respectively, a concordant pair is given by $\text{sign}(a_f - b_f) = \text{sign}(c_a - c_b)$ and a discordant pair is given by $\text{sign}(a_f - b_f) = -\text{sign}(c_a - c_b)$. A positive τ_f indicates that the fth connectivity measure increases in the patient population and vice versa for a negative τ_f. The absolute value of τ_f is used as a measure of relevance of a connection.

ReliefF:

The Relief feature selection introduced by [40] has been popularly used in many feature selection tasks. Many modifications of this algorithm have been proposed. We use the ReliefF feature selection which is more robust to noise and can be generalized to multi-class problems.

For a two class problem, ReliefF updates the rank of an attribute by assigning a high score to those attributes that are different between the classes. This is done by using two sets of n nearest neighbors to a randomly sampled instance. One set of neighbors are those that belong to the same class as the instance and the other set belongs to the second

class. Further details about the algorithm can be found in [40,41].

Information Gain Attribute selection (IGAS):

Information gain is an entropy-based feature selection technique that evaluates an attributes quality by measuring the gain in information with respect to a class, c [42]. This is done by measuring the gain in entropy of class, c, when knowledge of attribute, f, is used.

$$IG(c,f) = H(c) - H(c \mid f) \quad (4)$$

Here, IG is the information gain and H is the entropy.

In this study, we used 100 different train/test separations to investigate generalizability of the classifiers. Since the feature ranking was based on the training data, we obtain 100 different feature rankings for the dataset with slightly different scores for each interaction measure across iterations. We obtained *consensus features* scores by the average of scores across iterations for all connectivity measures [12]. Such features provide meaningful insights about how connectivity between regions are affected as a consequence of a disease.

3.2.2. Classifiers

To test the discriminative ability of the ranked features, using the above mentioned feature selection approaches, classification was performed. The AdaBoost [43] and Random Forests [44] classifier were used. AdaBoost and Random Forests are both ensemble classifiers that use an ensemble of weak classifiers to produce a strong classifier. Weak classifiers are those that can give accuracies just above random chance. The AdaBoost classifier consisting of decision stump classifier is used in this study. Random forests are comprised of a number of decision trees on different bootstraps of the training dataset. Generally, the parameters of the classifier, hyperparameters, are selected by dividing the dataset into train, development and test sets. The development set is used to select the hyperparameters. However, limited by the sample size in this study, dividing the dataset into train, development and test sets, would greatly reduce the data size used for training. Thus, to we use the default parameter settings from WEKA to compare performance of MCA-LM and correlation.

The WEKA [45] implementation of ReliefF, Information Gain Attribute selection (IGAS), AdaBoost and Random Forests were imported into MATLAB 2016 and used in our analysis. A flowchart of the steps involved in the analysis is provided in Fig. 1.

3.2.3. Classification performance metrics

Strict separation between training and testing data was carried out, with 90 % /10% train/test separation within an iterative cross-validation scheme. Both feature selection and training of classifier was performed on the training data. The data set was divided in such a way that the classifier received an equal number of subjects from both groups during training in order to prevent bias towards a particular class. Furthermore, the test set had at least one instance from both classes. The 100 splits were created ensuring no redundant train/test splits. The classifier performance was evaluated using accuracy of classification and the Area under the Receiver Operator Characteristic Curve (AUC). An AUC of 1 indicated perfect classification while an AUC of 0.5 indicates random classification.

4. Results

4.1. Classification performance

Figs. 2 and 3 show the plots of the AUC and accuracy values for 100 different training/test splits of the data. In all six combinations, the superiority of MCA-LM as compared to correlation can be clearly seen. It is also interesting to note that increasing the number of features does not improve performance, especially for the random forest classifier. Of the three feature selection approaches investigated, Kendall's τ performs the best for both classifiers. With MCA-LM connectivity measures as features, the mean AUC for AdaBoost classifier varies from 0.89 to 0.78 and mean accuracy varies from 0.86 to 0.72, while with Random forests, AUC varies from 0.89 to 0.67 and accuracy from 0.85 to 0.64 across different feature selection techniques and number of features retained. With correlation measures as features, the mean AUC for AdaBoost classifier varies from 0.86 to 0.67 and mean accuracy varies from 0.81 to 0.65, while with Random forests, AUC varies from 0.86 to 0.62 and accuracy from 0.82 to 0.62 across different feature selection techniques and number of features retained. The black dots corresponding to the number of features selected indicates if MCA-LM and correlation are significantly ($p < 0.01$) different from each other for

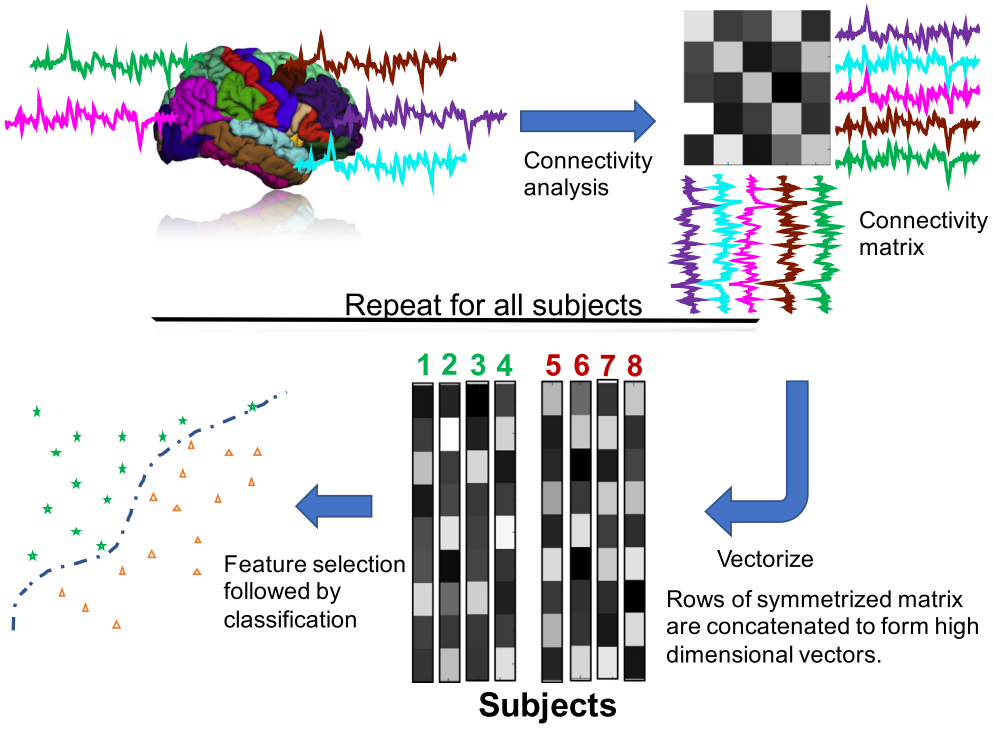

Fig. 1. Flowchart of steps involved in classifying healthy controls and patients presenting with HAND symptoms using resting-state fMRI. First, the resting-state fMRI data is preprocessed following which regional time-series are extracted. Subsequently, we obtain the connectivity matrix using either MCA-LM or correlation for each subject. These vectorized matrices are representative feature for every subject which are used to train and test the classifier.

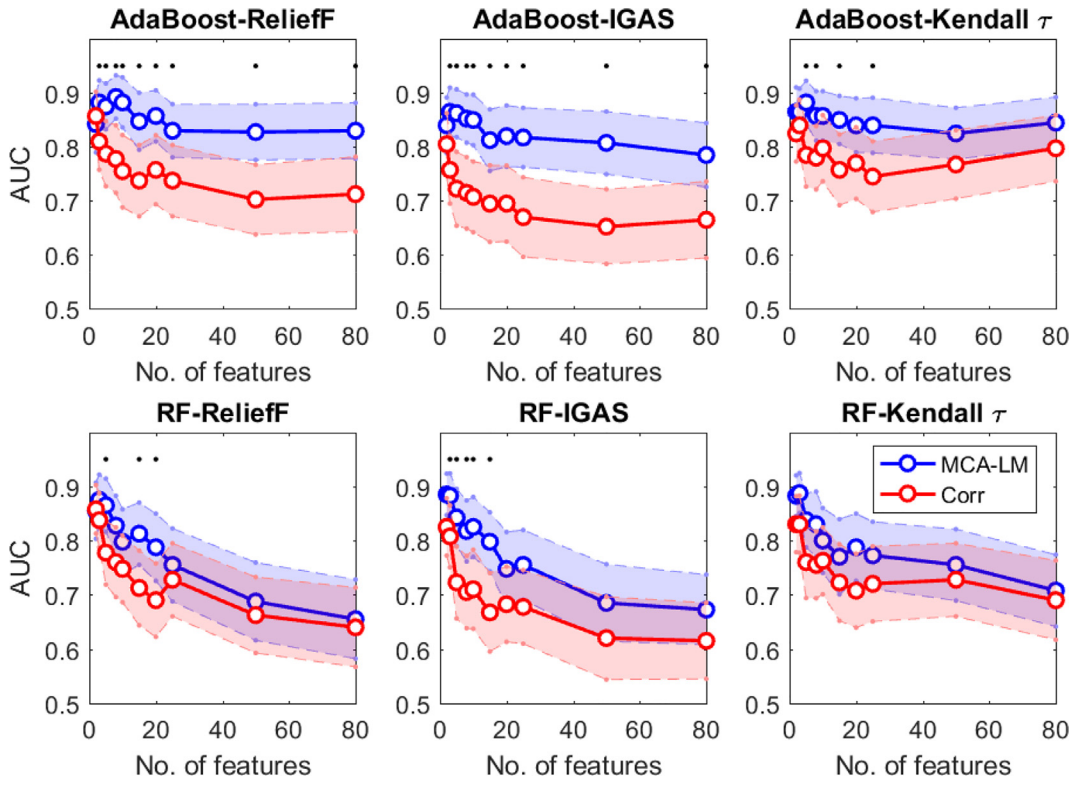

Fig. 2. Plot of AUC for the three feature selection approaches using two classifiers. Shaded regions above and below each solid line, corresponding to the mean AUC, represents the 95% confidence interval of the AUC value. The general trend observed here is that MCA-LM outperforms correlation. The black dots corresponding to the number of features selected indicates if MCA-LM and correlation are significantly ($p < 0.01$) different from each other for the given number of features.

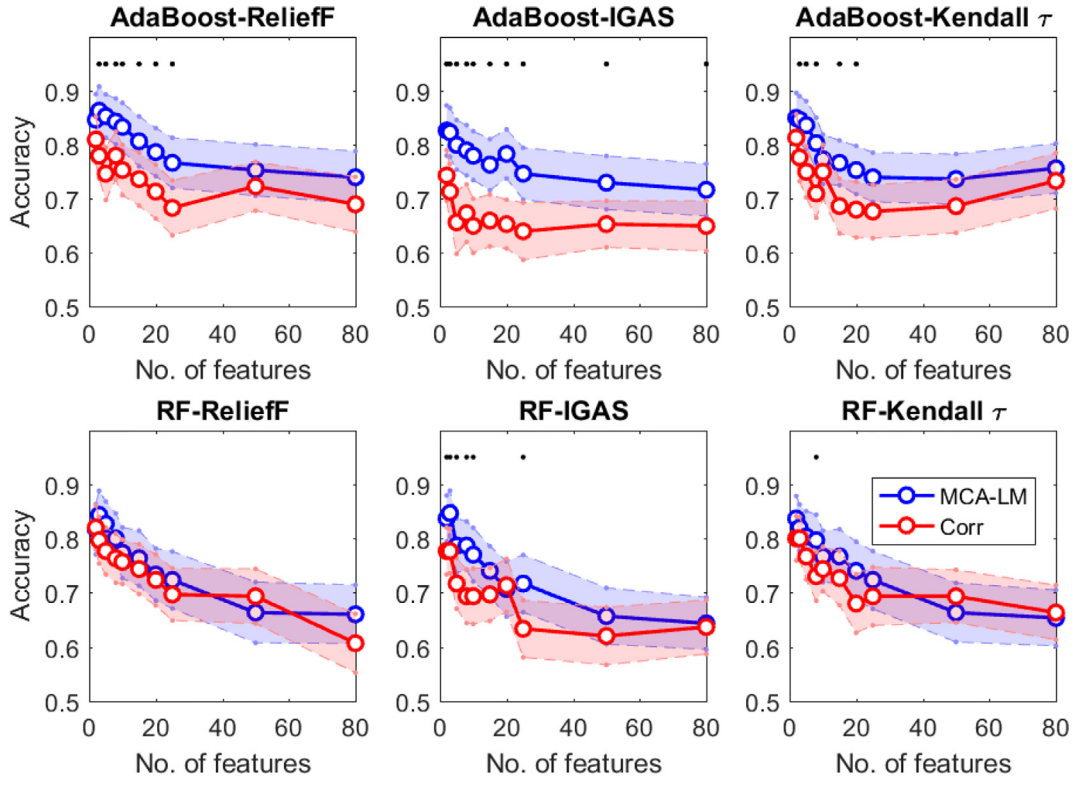

Fig. 3. Plot of accuracy for the three feature selection approaches using two classifiers. Shaded regions above and below each solid line, corresponding to the mean accuracy, represents the 95% confidence interval of the accuracy value. The general trend observed here is that MCA-LM outperforms correlation. The black dots corresponding to the number of features selected indicates if MCA-LM and correlation are significantly ($p < 0.01$) different from each other for the given number of features.

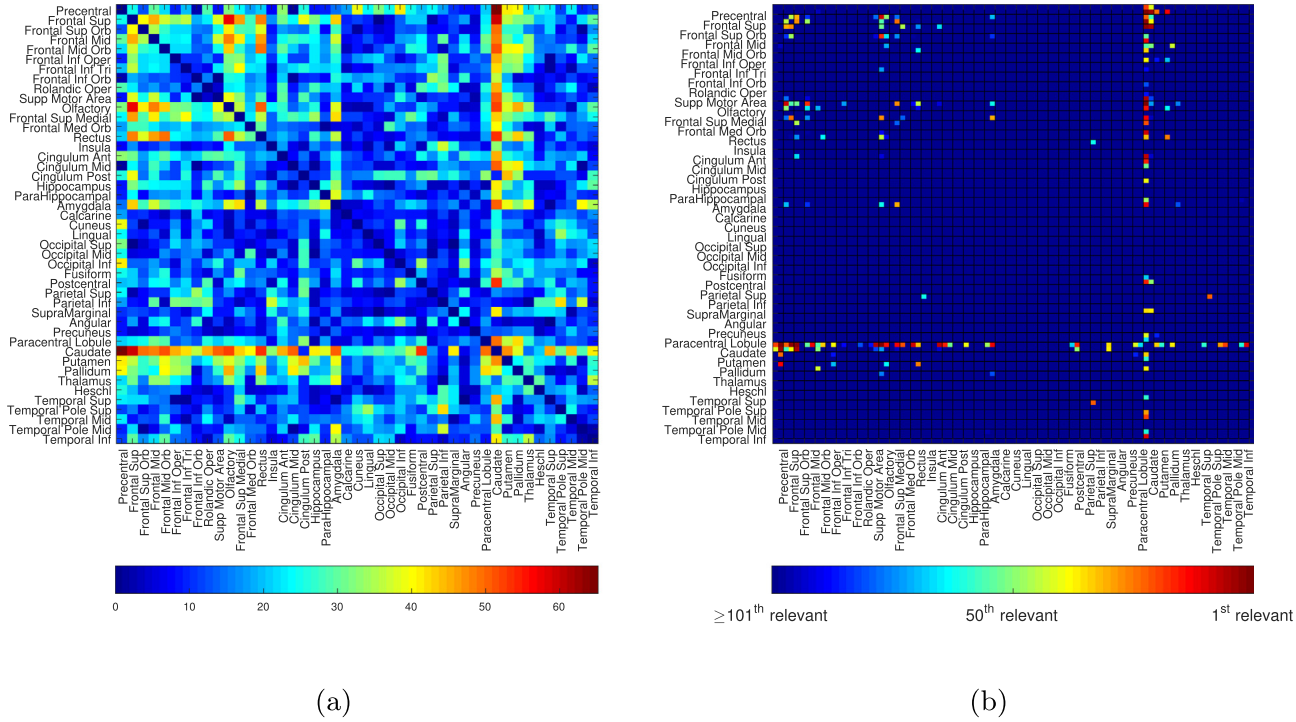

Fig. 4. Consensus feature scores using Kendall's τ feature section for MCA-LM (left) and plot of the 100 most relevant connections obtained from the consensus features scores (right). Left: Colors indicate strength of the score assigned to each feature. Warmer colors represent an increase in the interaction strength in patients with HAND symptoms as compared to healthy controls and vice versa with respect to cooler colors. For the sake of image clarity, the left and right hemisphere's are averaged to give one value. Right: Ranking of the absolute value of the consensus features gives the most relevant connections. The left and right hemisphere part of each region are within the square of the grid, where the regions name is on the x- and y-axis. Interactions between the caudate and most regions are affected. Additionally, the fronto-striatal connectivity is different between groups.

the given number of features. Here, we observe that MCA-LM is significantly better than correlation for different combinations of feature selection techniques. Sensitivity and specificity (supplementary material) also demonstrate the superiority of MCA-LM over traditional correlation based approaches.

4.2. Changes in resting-state connectivity in subjects with HAND symptoms

MCA-LM with Kendall's τ features is the most discriminative amongst both connectivity analysis and all feature selection combinations as evident by the high AUC and accuracy values (Figs. 2 and 3). Hence, we investigate interactions that were most important in discriminating between the two subject groups. To this end, consensus features scores [12] (described in Section 4) are used to produce relevance scores and ranking Fig. 4. Fig. 4a depicts the consensus feature scores. Here, the colors indicate the strength of the score to each feature assigned using Kendall's τ. Although we display scores calculated by Kendall's τ, similar features were selected by all the other feature selection approaches. Warmer colors in Fig. 4a represent those interactions that were very relevant to the task of discriminating the two groups and vice versa with respect to cooler colors. Studying Fig. 4a we see that the regions most affected by the viral infection of the brain are the caudate, putamen, pallidium and thalamus (basal ganglia). In addition, changes in the frontal cortex were observed. These regions have been shown to be affected by HIV infection of the brain. Fig. 4b is a plot of the 100 most relevant features in order of relevance where maroon indicates most relevant connection (i.e. highest consensus score) and dark blue indicates the 100th relevant connection. Here we see that interactions between the caudate and most other regions are very relevant.

5. Discussion

Based on our analysis, results suggest that MCA-LM outperforms conventionally used methods of correlation in the MVPA framework, consistently over a number of features, different feature selection techniques and different classifiers. This indicates that MCA-LM can capture meaningful information about network characteristics from brain activity data. Previously, on realistic simulations of fMRI data, it was demonstrated that MCA-LM can reproduce the underlying network in close agreement to the ground truth network structure [2]. It's ability can be attributed to the flexibility of its nonlinear modeling scheme. In addition to characterizing network structure well, MCA-LM seems to be able to pick up subtle differences in the underlying network structure between the two groups of subjects as compared to correlation. Hence, the improved classification performance.

Since the MVPA framework with MCA-LM, feature selection followed by classification, provides good classification results, we investigated the features selected to study interactions found to be relevant. Feature selection was adopted since it can reveal regional interactions that are the most discriminative. Fig. 4a shows the Kendall's τ coefficient scores for all the regions. The connectivity of the caudate region within the basal ganglia to most other regions is altered in our cohort which is in line with previous studies. Dysfunction in the caudate can possibly lead to cognitive deficits affecting learning, working memory and executive functioning [35]. Furthermore, it has been previously shown that metabolic dysfunction [46] and histologic abnormalities [47] have been detected in the basal ganglia of patients with HIV infection.

We were also interested in taking a closer look at the most relevant features estimated for the connectivity matrices generated using MCA-LM. Fig. 4b shows plots of the 100 most relevant connections obtained using Kendall's τ feature selection approaches on MCA-LM connectivity

matrices represented as a matrix of relevant interactions. All three feature selection techniques pick up similar sets of relevant features for each of the connectivity analysis approaches. Interactions between the caudate and most regions are very relevant. Particularly, the fronto-striatal connectivity seems to be affected. These interactions play a role in executive functioning and have been implicated in the progression of HAND previously [48]. Additionally, the connectivity within the superior frontal regions and also from these regions to the supplementary motor areas are relevant for distinguishing the subjects. The good classification results and meaningful neuroimaging-derived biomarkers motivates use of such nonlinear models, especially to extract clinically relevant biomarkers.

Limitations and future work.

In this study, we obtain measures of connectivity between regions using MCA-LM. Our results suggest that MCA-LM outperforms conventionally used correlation in the MVPA framework. However, in the future it would also be interesting to evaluate MCA-LM the with other nonlinear techniques such as [49,50]. Furthermore, we acknowledge that this study is limited by the sample size. In this work, we obtain relevant features, corresponding to regional interactions, that are different between healthy controls and individuals with HIV associated neurocognitive disorder. However, to derive statistically meaningful differences between regional interactions amongst healthy individuals and individuals presenting with symptoms of HAND a more robust, multi-site analysis with larger number of samples should be carried out [51]. Additionally, it would be of interest to conduct a longitudinal study with HIV individuals who do not have symptoms of neurodegeneration initially but develop them over time. It would be of great value to the scientific community if such a framework can perform early detection of HAND, since neuronal level changes can manifest much before cognitive symptoms appear, [52,53].

6. Conclusion

In this paper we investigate the effectiveness of Mutual Connectivity Analysis (MCA) with Local Models to quantify underlying non-linear interaction between resting-state brain activities across regions and subsequently, discriminate between healthy controls and patients with HAND. We also compare the effectiveness of MCA-LM against conventionally used functional connectivity analysis such as correlation in classifying the two groups. In addition, we study the changes in interaction between brain regions, as defined based on the AAL template, as a result of neurodegeneration on account of HIV infecting the brain.

Each subject is represented by a high-dimensional vector of features, where, the features are pair-wise interaction measures quantified by MCA-LM. Similarly, correlation was used as another measure of time-series interaction. As such, all the subjects were represented by two sets of features, one derived using MCA-LM and the other derived with correlation. Good classification results with MCA-LM indicates that such a measure of connectivity quantifies interaction between different brain-regions well. Improved performance as compared with correlation suggests that MCA-LM carries more meaningful and clinical useful information. MCA-LM outperforms correlation for all six different combinations of feature selection and classification for varying number of selected features. Feature selection on connectivity measures help select the most discriminant connections giving an idea of changes occurring at a local level. The fronto-striatal circuitry seems to be particularly affected in subjects with HAND.

In conclusion, MCA-LM method has the potential to provide clinically useful information about how the underlying dynamics of the resting human brain differs between subjects presenting with symptoms of HAND and healthy controls. Such an exploration can aid in uncovering neural mechanisms underlying development of symptoms of HAND. This may be instrumental in providing additional information to advance understanding of the pathophysiology of HAND. Besides HIV related brain disease, we conjecture that our method may be applicable to serve as a diagnostic biomarker for other neurologic conditions as well.

Acknowledgement

This work was funded by the National Institutes of Health (NIH) Award R01-DA-034977 and R01 MH099921. The content is solely the responsibility of the authors and does not necessarily represent the official views of the National Institute of Health. This work was conducted as a Practice Quality Improvement (PQI) project related to American Board of Radiology (ABR) Maintenance of Certificate (MOC) for Prof. Dr. Axel Wismüller. The authors would like to thank Prof. Dr. Herbert Witte of Bernstein Group for Computational Neuroscience, Jena, Institute of Medical Statistics, Computer Science and Documentation, Jena University Hospital, Friedrich Schiller University, Jena, Germany, Dr. Oliver Lange and Prof. Dr. Maximilian F. Reiser of the Institute of Clinical Radiology, Ludwig Maximilian University, Munich, Germany for their support.

References

[1] Friston KJ, Mechelli A, Turner R, Price CJ. Nonlinear responses in fMRI: the balloon model, Volterra kernels, and other hemodynamics. NeuroImage 2000;12(4):466–77.
[2] DSouza AM, Abidin AZ, Chockanathan U, Schifitto G, Wismüller A. Mutual connectivity analysis of resting-state functional mri data with local models. NeuroImage 2018.
[3] Sugihara G, May R, Ye H, Hsieh C-h, Deyle E, Fogarty M, et al. Detecting causality in complex ecosystems. science 2012;338(6106):496–500.
[4] Wismüller A, Abidin AZ, DSouza AM, Nagarajan MB. Mutual connectivity analysis (mca) for nonlinear functional connectivity network recovery in the human brain using convergent cross-mapping and non-metric clustering. Advances in self-organizing maps and learning vector quantization. Springer; 2016. p. 217–26.
[5] Lombardi A, Guccione P, Mascolo L. Analysis of fMRI data using the complex systems approach. 20th IMEKO TC-4 international symposium on measurements of electrical quantities, Benevento. 2014. p. 15–7.
[6] Gautama T, Mandic DP, Van Hulle MM. Signal nonlinearity in fMRI: a comparison between BOLD and MION. IEEE Trans Med Imaging 2003;22(5):636–44.
[7] Minati L, Chiesa P, Tabarelli D, D'Incerti L, Jovicich J. Synchronization, non-linear dynamics and low-frequency fluctuations: analogy between spontaneous brain activity and networked single-transistor chaotic oscillators. Chaos: An Interdisciplinary Journal of Nonlinear Science 2015;25(3):033107.
[8] Gultepe E, He B. A linear/nonlinear characterization of resting state brain networks in fMRI time series. Brain Topogr 2013;26(1):39–49.
[9] Xie X, Cao Z, Weng X. Spatiotemporal nonlinearity in resting-state fMRI of the human brain. Neuroimage 2008;40(4):1672–85.
[10] Norman KA, Polyn SM, Detre GJ, Haxby JV. Beyond mind-reading: multi-voxel pattern analysis of fMRI data. Trends Cogn Sci 2006;10(9):424–30.
[11] Craddock RC, Holtzheimer PE, Hu XP, Mayberg HS. Disease state prediction from resting state functional connectivity. Magn Reson Med 2009;62(6):1619–28.
[12] Zeng L-L, Shen H, Liu L, Wang L, Li B, Fang P, et al. Identifying major depression using whole-brain functional connectivity: a multivariate pattern analysis. Brain 2012;135(5):1498–507.
[13] Savio A, Graña M. Local activity features for computer aided diagnosis of schizophrenia on resting-state fMRI. Neurocomputing 2015;164:154–61.
[14] Bleich-Cohen M, Jamshy S, Sharon H, Weizman R, Intrator N, Poyurovsky M, et al. Machine learning fMRI classifier delineates subgroups of schizophrenia patients. Schizophr Res 2014;160(1):196–200.
[15] Drysdale AT, Grosenick L, Downar J, Dunlop K, Mansouri F, Meng Y, et al. Resting-state connectivity biomarkers define neurophysiological subtypes of depression. Nat Med 2017;23(1):28.
[16] Shen H, Wang L, Liu Y, Hu D. Discriminative analysis of resting-state functional connectivity patterns of schizophrenia using low dimensional embedding of fMRI. Neuroimage 2010;49(4):3110–21.
[17] Ardekani BA, Tabesh A, Sevy S, Robinson DG, Bilder RM, Szeszko PR. Diffusion tensor imaging reliably differentiates patients with schizophrenia from healthy volunteers. Hum Brain Mapp 2011;32(1):1–9.
[18] Zhou J, Greicius MD, Gennatas ED, Growdon ME, Jang JY, Rabinovici GD, et al. Divergent network connectivity changes in behavioural variant frontotemporal dementia and Alzheimer's disease. Brain 2010;133(5):1352–67.
[19] Balsters JH, Mantini D, Apps MA, Eickhoff SB, Wenderoth N. Connectivity-based parcellation increases network detection sensitivity in resting state fMRI: an investigation into the cingulate cortex in autism. NeuroImage: Clinical 2016;11:494–507.
[20] Abidin AZ, DSouza AM, Nagarajan MB, Wang L, Qiu X, Schifitto G, et al. Alteration of brain network topology in HIV-associated neurocognitive disorder: a novel functional connectivity perspective. NeuroImage: Clinical 2018;17:768–77.
[21] Thomas JB, Brier MR, Snyder AZ, Vaida FF, Ances BM. Pathways to neurodegeneration effects of HIV and aging on resting-state functional connectivity. Neurology

2013;80(13):1186–93.
[22] du Plessis L, Paul RH, Hoare J, Stein DJ, Taylor PA, Meintjes EM, et al. Resting-state functional magnetic resonance imaging in clade C HIV: within-group association with neurocognitive function. J Neurovirol 2017;23(6):875–85.
[23] Zhuang Y, Qiu X, Wang L, Ma Q, Mapstone M, Luque A, et al. Combination antiretroviral therapy improves cognitive performance and functional connectivity in treatment-naïve HIV-infected individuals. J Neurovirol 2017;23(5):704–12.
[24] Antinori A, Arendt G, Becker J, Brew B, Byrd D, Cherner M, et al. Updated research nosology for HIV-associated neurocognitive disorders. Neurology 2007;69(18):1789–99.
[25] Zeng L-L, Wang D, Fox MD, Sabuncu M, Hu D, Ge M, et al. Neurobiological basis of head motion in brain imaging. Proc Natl Acad Sci 2014;111(16):6058–62.
[26] Van Dijk KR, Sabuncu MR, Buckner RL. The influence of head motion on intrinsic functional connectivity MRI. Neuroimage 2012;59(1):431–8.
[27] Jenkinson M, Smith S. A global optimisation method for robust affine registration of brain images. Med Image Anal 2001;5(2):143–56.
[28] Sikka S, Cheung B, Khanuja R, Ghosh S, Yan C, Li Q, et al. Towards automated analysis of connectomes: the configurable pipeline for the analysis of connectomes (C-PAC). 5th INCF congress of neuroinformatics, Munich, Germany. vol. 10. 2014.
[29] Smith SM, Jenkinson M, Woolrich MW, Beckmann CF, Behrens TE, Johansen-Berg H, et al. Advances in functional and structural MR image analysis and implementation as FSL. NeuroImage 2004;23(Suppl. 1):S208–19. https://doi.org/10.1016/j.neuroimage.2004.07.051.
[30] Wismüller A, Lange O, Dersch DR, Leinsinger GL, Hahn K, Pütz B, et al. Cluster analysis of biomedical image time-series. International Journal of Computer Vision 2002;46(2):103–28. https://doi.org/10.1023/A:1013550313321.
[31] Tzourio-Mazoyer N, Landeau B, Papathanassiou D, Crivello F, Etard O, Delcroix N, et al. Automated anatomical labeling of activations in SPM using a macroscopic anatomical parcellation of the MNI MRI single-subject brain. Neuroimage 2002;15(1):273–89.
[32] Wang X, Foryt P, Ochs R, Chung J-H, Wu Y, Parrish T, et al. Abnormalities in resting-state functional connectivity in early human immunodeficiency virus infection. Brain Connect 2011;1(3):207–17.
[33] Thomas JB, Brier MR, Ortega M, Benzinger TL, Ances BM. Weighted brain networks in disease: centrality and entropy in human immunodeficiency virus and aging. Neurobiol Aging 2015;36(1):401–12.
[34] Clifford DB, Ances BM. HIV-associated neurocognitive disorder. Lancet Infect Dis 2013;13(11):976–86.
[35] Ellis R, Langford D, Masliah E. HIV and antiretroviral therapy in the brain: neuronal injury and repair. Nat Rev Neurosci 2007;8(1):33.
[36] Takens F. Detecting strange attractors in turbulence. Dynamical systems and turbulence, Warwick 1980. Springer; 1981. p. 366–81.
[37] Ruelle D. Chaotic evolution and strange attractors. vol. 1. Cambridge University Press; 1989.
[38] Deyle ER, Sugihara G. Generalized theorems for nonlinear state space reconstruction. PLoS One 2011;6(3):e18295.
[39] M. G. Kendall, Rank correlation methods.
[40] Kononenko I. Estimating attributes: analysis and extensions of relief. European conference on machine learning. Springer; 1994. p. 171–82.
[41] Kononenko I, Šimec E, Robnik-Šikonja M. Overcoming the myopia of inductive learning algorithms with relieff. Applied Intelligence 1997;7(1):39–55.
[42] E. B. Hunt, J. Marin, P. J. Stone, Experiments in induction.
[43] Freund Y, Schapire RE. A decision-theoretic generalization of on-line learning and an application to boosting. Journal of Computer and System Sciences 1997;55(1):119–39.
[44] Ho TK. Random decision forests. Document analysis and recognition, 1995. Proceedings of the third international conference on. vol. 1. IEEE; 1995. p. 278–82.
[45] Hall M, Frank E, Holmes G, Pfahringer B, Reutemann P, Witten IH. The WEKA data mining software: an update. ACM SIGKDD Explorations Newsletter 2009;11(1):10–8.
[46] Wenserski F, von Giesen H-J, Wittsack H-J, Aulich A, Arendt G. Human immunodeficiency virus 1–associated minor motor disorders: perfusion-weighted MR imaging and 1H MR spectroscopy. Radiology 2003;228(1):185–92.
[47] Archibald SL, Masliah E, Fennema-Notestine C, Marcotte TD, Ellis RJ, McCutchan JA, et al. Correlation of in vivo neuroimaging abnormalities with postmortem human immunodeficiency virus encephalitis and dendritic loss. Arch Neurol 2004;61(3):369–76.
[48] Melrose RJ, Tinaz S, Castelo JMB, Courtney MG, Stern CE. Compromised frontostriatal functioning in HIV: an fMRI investigation of semantic event sequencing. Behav Brain Res 2008;188(2):337–47.
[49] Lombardi A, Tangaro S, Bellotti R, Bertolino A, Blasi G, Pergola G, et al. A novel synchronization-based approach for functional connectivity analysis. Complexity 2017;2017.
[50] Liao W, Marinazzo D, Pan Z, Gong Q, Chen H. Kernel granger causality mapping effective connectivity on fMRI data. IEEE Trans Med Imaging 2009;28(11):1825–35.
[51] Zeng L-L, Wang H, Hu P, Yang B, Pu W, Shen H, et al. Multi-site diagnostic classification of schizophrenia using discriminant deep learning with functional connectivity MRI. EBioMedicine 2018;30:74–85.
[52] Cysique LA, Brew BJ. Prevalence of non-confounded HIV-associated neurocognitive impairment in the context of plasma HIV RNA suppression. J Neurovirol 2011;17(2):176–83.
[53] Holt JL, Kraft-Terry SD, Chang L. Neuroimaging studies of the aging HIV-1-infected brain. J Neurovirol 2012;18(4):291–302.